Effect of acyl chain unsaturation on the conformation of model diacylglycerols: a computer modeling study

Kenneth R. Applegate and John A. Glomset

Regional Primate Research Center, Departments of Biochemistry and Medicine, and Howard Hughes Medical Institute Laboratories, SL-15, University of Washington, Seattle, WA 98195

Abstract In a previous modeling study we identified an angle iron-shaped conformation of docosahexaenoic acid and showed that an *sn*-1-stearoyl diacylglycerol (DG) that contained an *sn*-2-docosahexaenoyl group in this conformation could adopt a highly regular shape. In the present study we compared the properties of this DG with those of *sn*-1-stearoyl DGs that contained other unsaturated fatty acyl groups in the *sn*-2 position. The major findings were that: *1*) *sn*-1-stearoyl DGs that contain polyenoic fatty acids in the *sn*-2 position can assume regular shapes, and *2*) these shapes differ depending on the location of the double bonds. *sn*-2-Polyenoic fatty acyl groups with a double bond sequence that begins close to the carboxyl ester bond are associated with one type of regular shape, while *sn*-2-polyenoic fatty acyl groups with a double bond sequence that begins toward the middle of the chain are associated with another. Such shapes would not have been predicted by current ideas relating membrane fluidity to unsaturation. In contrast, another finding of the present study, that *sn*-1-stearoyl-2-oleoyl DG can adopt, at best, only a highly irregular shape is in good agreement with the results of previous investigators. —**Applegate, K. R., and J. A. Glomset.** Effect of acyl chain unsaturation on the conformation of model diacylglycerols: a computer modeling study. *J. Lipid Res.* 1991. **32:** 1635–1644.

Supplementary key words docosahexaenoic acid • arachidonic acid • eicosatrienoic acid • stearic acid • linoleic acid • linolenic acid • oleic acid

The phospholipids of animal cell membranes typically contain high proportions of polyunsaturated fatty acids. The structural role of these fatty acids remains to be determined, but they are generally believed to increase membrane fluidity. One reason for this belief is that the single *cis* double bond in oleic acid decreases the fatty acid's melting point and interferes with its packing in monolayers. The *cis* double bond clearly interrupts the regular *trans/trans* structure of the saturated acyl chain. However, in a molecular modeling study of docosahexaenoic acid, we provided evidence that a methylene-interrupted sequence of *cis* double bonds need not have this effect (1). Use of the MM2 molecular mechanics program of Allinger (2–4) demonstrated that two or more methylene-interrupted *cis* double bonds can assume an "angle-iron-shaped" conformation, in which the double bond directions are parallel and alternate double bond planes are perpendicular to one another. In docosahexaenoic acid this double bond conformation is associated with a straight chain axis that would seem likely to promote rather than prevent acyl chain packing. Having obtained this evidence regarding docosahexaenoic acid, it seemed reasonable to ask whether shorter sequences of methylene-interrupted *cis* double bonds in other polyenoic fatty acids might have a similar effect.

To address this question we decided to extend our modeling study to include a series of diacylglycerols (DGs) that contained stearic acid in the *sn*-1 position and different unsaturated fatty acids in the *sn*-2 position. We used MM2 to optimize conformations of these DGs that contained angle-iron-shaped polyenoic segments. In addition, we sought to identify related structural determinants that might affect the packing of diacyl phospholipids in membranes. In this report we describe the distinctive features of these conformations. In a companion article (5) we describe their effects on the packing of DGs in simulated monolayers.

METHODS

Computer resources

As described previously (1), we used an integrated biomedical package, PROPHET, because of its molecular

Abbreviations: DG, diacylglycerol; 18:0/18:0 DG, *sn*-1,2-distearoylglycerol; 18:0/18:1(n-9) DG, *sn*-1-stearoyl-2-oleoylglycerol; 18:0/18:2(n-6) DG, *sn*-1-stearoyl-2-linoleoylglycerol; 18:0/18:3(n-3) DG, *sn*-1-stearoyl-2-linolenoylglycerol; 18:0/20:3(n-9) DG, *sn*-1-stearoyl-2-(5,8,11)-eicosatrienoylglycerol; 18:0/20:4(n-6) DG, *sn*-1-stearoyl-2-arachidonoylglycerol; 18:0/22:6(n-3) DG, *sn*-1-stearoyl-2-docosahexaenoylglycerol; 12:0/12:0 DG, *sn*-1,2-dilauroylglycerol; PE, phosphatidylethanolamine.

TABLE 1. Dihedral angles of backbone bonds for optimized conformations of DGs

Dihedral Atoms[b]	Bond[c]	Type 1[a]			Type 2			Type 3
		18:0/ 22:6(n-3)	18:0/ 20:4(n-6)	18:0/ 20:3(n-9)	18:0/ 18:0	18:0/ 18:2(n-6)	18:0/ 18:3(n-3)	18:0/ 18:1(n-9)
H11A-O11-C1-C2	α1	-179.3	-179.8	179.9	-177.9	-177.6	-178.4	-178.0
O11-C1-C2-C3	θ1	177.1	179.2	179.9	-59.8	178.1	176.2	178.7
O11-C1-C2-O21	θ2	-62.9	-62.3	-62.5	61.1	-62.4	-64.3	-61.7
C1-C2-C3-O31	θ3	-170.6	-170.6	179.9	-179.9	177.5	175.6	-178.7
O31-C3-C2-O21	θ4	68.7	70.8	72.3	59.4	58.0	56.3	60.7
C1-C2-O21-C21	β1	99.0	109.1	106.2	129.9	140.6	140.7	91.4
C2-O21-C21-C22	β2	177.2	-172.8	-173.4	170.5	171.9	176.3	178.6
O21-C21-C22-C23	β3	-90.1	-102.8	-105.1	-140.1	-145.0	-144.7	-110.1
C21-C22-C23-C24	β4	68.6	52.8	57.0	68.9	61.3	60.1	80.7
C22-C23-C24-C25	β5	-171.6	-94.7	-93.4	176.3	170.2	170.3	177.9
C23-C24-C25-C26	β6	0.0	-117.1	-119.7	178.8	-175.7	-176.7	-176.8
C24-C25-C26-C27	β7	121.7	-2.0	-1.5	177.7	167.8	167.3	174.2
C25-C26-C27-C28	β8	120.2	-110.5	-113.9	179.7	-170.0	-172.7	-178.0
C26-C27-C28-C29	β9	-0.1	-125.1	-121.7	178.6	-83.1	-79.9	-73.9
C27-C28-C29-C210	β10	-120.6	-0.7	-0.5	179.9	-139.1	-133.8	-121.8
C28-C29-C210-C211	β11	-122.4	126.1	138.6	179.3	2.3	0.7	0.6
C29-C210-C211-C212	β12	-0.1	116.4	98.3	179.7	-122.4	-116.8	-113.3
C210-C211-C212-C213	β13	121.1	0.0	-0.2	179.8	-120.1	-124.2	-178.8
C211-C212-C213-C214	β14	121.5	-124.3	-154.4	179.8	0.7	0.3	177.6
C212-C213-C214-C215	β15	-0.2	-121.0	-68.5	-179.8	-143.5	126.3	-178.2
C213-C214-C215-C216	β16	-122.5	0.3	-166.6	-179.9	-84.6	120.4	178.8
C214-C215-C216-C217	β17	-122.8	140.3	178.1	-179.8	-174.5	0.2	-178.8
C215-C216-C217-C218	β18	-0.5	71.2	-173.5	-179.7	173.3	-90.5	179.6
C216-C217-C218-C219	β19	118.1	176.2	178.1	-179.8	178.3	-179.8	-179.8
C217-C218-C219-C220	β20	122.8	-73.2	-176.3				
C218-C219-C220-C221	β21	-0.5	-178.4	-179.4				
C219-C220-C221-C222	β22	-91.5						
C220-C221-C222-H222A	β23	-61.7						

TABLE 1. (contd)

Dihedral Atoms	Bond	Type 1			Type 2			Type 3
		18:0/ 22:6(n-3)	18:0/ 20:4(n-6)	18:0/ 20:3(n-9)	18:0/ 18:0	18:0/ 18:2(n-6)	18:0/ 18:3(n-3)	18:0/ 18:1(n-9)
C2-C3-O31-C31	γ1	-162.0	-165.9	-171.4	173.3	173.7	179.5	-176.7
C3-O31-C31-C32	γ2	-177.8	-173.1	-173.3	174.4	172.8	175.1	174.4
O31-C31-C32-C33	γ3	-177.1	-169.4	-159.9	176.0	178.5	169.8	-171.2
C31-C32-C33-C34	γ4	-175.6	179.8	-178.0	177.5	178.0	177.6	175.8
C32-C33-C34-C35	γ5	-179.7	-179.5	179.3	178.6	178.0	178.4	-179.9
C33-C34-C35-C36	γ6	-177.8	-178.3	-176.1	178.6	-179.1	179.0	-178.5
C34-C35-C36-C37	γ7	-179.2	-178.7	179.7	179.2	178.4	179.5	-179.4
C35-C36-C37-C38	γ8	-179.6	-177.0	-175.5	179.3	-178.0	179.9	179.9
C36-C37-C38-C39	γ9	-179.5	178.1	177.4	179.6	-176.0	177.3	-179.0
C37-C38-C39-C310	γ10	179.0	-176.0	-179.0	179.9	177.2	178.5	-179.9
C38-C39-C310-C311	γ11	-180.0	177.8	178.6	179.7	-178.7	177.7	-179.4
C39-C310-C311-C312	γ12	179.0	-172.6	179.1	179.9	177.5	179.0	-179.7
C310-C311-C312-C313	γ13	-179.2	-171.4	-178.2	179.9	178.5	179.3	-180.0
C311-C312-C313-C314	γ14	-179.0	173.2	177.1	179.9	-179.4	-178.9	-179.9
C312-C313-C314-C315	γ15	179.6	-174.8	-177.1	-180.0	179.6	179.7	179.7
C313-C314-C315-C316	γ16	175.3	172.7	176.4	179.6	-177.3	-178.5	179.8
C314-C315-C316-C317	γ17	-179.4	174.9	-178.4	179.9	-178.0	179.9	179.6
C315-C316-C317-C318	γ18	-179.9	178.5	178.4	179.6	-178.1	-179.1	179.6
C316-C317-C318-H318A	γ19	-179.9	177.9	-179.8	179.8	-179.1	-179.9	179.8

Dihedral angles are measured in degrees clockwise from the eclipsed (*cis*) position. Portions of the table are outlined to show specific geometric regions of the molecules. Bond sequences defining the 90° bend in the *sn*-2 chain are contained within the heavy single-line borders. Double bonds and angle-iron sequences are found within the double-line borders. Transitional regions between saturated and double bond regions are outlined with dotted borders.

[a]DG conformation types as defined in the text.

[b]Atom-naming conventions are those of Sundaralingam (21). The format Xm, (X = atomic symbol, m = 1,2,3), e.g., C2, labels atoms in the glyceryl moiety. The formats X1n, X2n, X3n label atoms in the *sn*-3 hydroxyl, *sn*-2, and *sn*-1 chains, respectively, where n is the atom index counted along the chain from the ester linkage, e.g., C318 for the 18th carbon of the *sn*-1 chain. Postfixes A,B,C distinguish hydrogen atoms bonded to the same backbone atom, e.g., H318A.

[c]α, β, and γ prefixes designate bonds in the *sn*-3 hydroxyl, *sn*-2, and *sn*-1 chains, while θ refers to the glyceryl moiety.

modeling capabilities. PROPHET was developed by BBN Systems and Technology, Cambridge, MA, under sponsorship of the NIH National Center for Research Resources. For early modeling we used PROPHET I running on a BBN mainframe computer. In later phases we used PROPHET II on a local Sun 3/60 workstation running under Unix (6). In addition, we performed some calculations on the Cray X/MP and Y/MP computers of the San Diego Supercomputer Center (SDSC) via NSFNet connections to the workstation.

Using previously described features of PROPHET (1), we created, manipulated, and analyzed molecular models. We used the PROPHET inferface program, CAMCRYST, to retrieve atomic coordinates for *sn*-1,2-dilauroyl phosphatidylethanolamine (PE) and other lipids from the Cambridge Crystal File (7) and to convert them to molecular models. We continued to use the PROPHET interface program MMP2MODEL (8) to the MM2/MMP2 molecular mechanics programs of Allinger to optimize molecular conformations (**Table 1**) and to calculate their steric energies (**Table 2**). PROPHET II used the 1987 version of MMP2 and its parameter set (9, 10). The initial 250-atom limit was later increased to 500 atoms (8). On the supercomputers, we used a 500-atom limit, 1985 modification by SDSC of the 1977 MM2 force field (2). All MM2 versions produced steric energies for DG models that agreed within a few tenths of a kilocalorie. Small differences in Van der Waals parameter sets accounted for remaining variability.

Models of individual DGs

We created models of DGs that contained an *sn*-1-stearoyl chain and *sn*-2-fatty acyl chains with 18 to 22 carbon atoms and various numbers of *cis* double bonds. NMR studies of phosphatidylserine, PE, phosphatidylcholine (11) and DG (12) in membranes showed that their conformation was similar to that of crystalline *sn*-1,2-dilauroyl PE (13). Therefore, we built the models by directly combining that glyceryl ester conformation with acyl chain models from our previous study, or with new chain models derived from modifications of the older ones. We paid particular attention to achieving extended forms of the *sn*-2 chains in which all chain segments were aligned as closely as possible. We also adjusted torsion angles in the original glyceryl ester moiety and in the acyl chains to bring the *sn*-1 and *sn*-2 chains into parallel, closely packed alignment. After the initial adjustments, we used MMP2 to "anneal" and refine each model to a minimum energy conformation.

sn-*1-Stearoyl-2-docosahexaenoyl DG.* The conformation described previously (1), originally assembled from minimized fragments, was used after reminimization as a whole by MMP2. It contained the angle-iron-shaped conformation of docosahexaenoic acid that we had identified, and incorporated our finding that the saturated *sn-1* chain may be rotated about its axis to a position that fits tightly in the groove of the *sn*-2 angle-iron conformation.

sn-*1-Stearoyl-2-arachidonoyl DG.* The model of *sn*-1-stearoyl-2-arachidonoyl DG created previously (1) had a much higher steric energy than the model of *sn*-1-stearoyl-2-docosahexaenoyl DG. This was traced to non-optimal bond geometries in a bulge created by the extra methylene before the beginning of the polyene sequence at the fifth carbon of the *sn*-2 chain. By adjusting bonds in the right angle bend, and by reversing the signs of all methylene torsion angles between the double bonds to produce a reflected configuration of the polyene sequence, we removed the bulge and produced a less strained bond geometry. Also, a somewhat irregular torsion angle sequence of *skew, gauche, trans, antigauche, trans* in the distal, saturated segment aligned it with the polyene segment

TABLE 2. Steric energy components for MMP2-optimized DG molecules

sn-1-Stearoyl-2-acyl-DG	Total Steric Energy	Compression	Bending	Stretch-Bend	VDW 1,4 Interactions	VDW Other Interactions	Torsional	Dipole
Type 1								
Docosahexaenoyl	30.81	2.60	12.41	1.03	31.02	−18.83	−3.55	6.13
Arachidonyl	34.26	2.99	12.99	1.24	31.12	−18.57	−1.11	5.61
Eicosatrienoyl (5,8,11)	29.71	2.80	10.39	1.13	32.12	−21.44	−0.86	5.57
Type 2								
Stearoyl	22.85	2.87	6.81	1.07	32.05	−20.26	−4.54	4.83
Linoleoyl	32.22	3.05	9.38	1.17	31.12	−15.96	−2.07	5.53
Linolenoyl	28.28	2.83	9.88	1.09	30.25	−17.68	−3.66	5.57
Type 3								
Oleoyl	29.64	2.88	8.22	1.07	31.54	−16.13	−3.88	5.95

All energies are in kcal/mole. Energy components correspond to the separate force-field components used by the MMP2 program. The compression, bending, and stretch-bend energies are calculated relative to "strain-free" bond lengths and bond angles defined in the MMP2 parameter set. Van der Waals energies are calculated using a modified Buckingham (exp-6) potential. The Van der Waals 1,4 energies represent non-bonded interactions between nearest-neighbors of bonded atoms, and are distinct from the torsional energies calculated from a superposition of 1-, 2-, and 3-fold rotational potentials about the bonds. Non-bonded energies between more distant atom pairs are summed under Van der Waals Other Interactions. Dipole energies are calculated using a bond-moment approximation. Differences in total steric energy among DGs arise mainly from strained bond angles, bond rotations away from positions of rotational energy minima, and differences in acyl chain length and interchain packing.

and made it better able to pack with the *sn*-1 chain than the original all-*trans* segment (Table 1).

sn-*1-Stearoyl-2-(5,8,11)-eicosatrienoyl DG.* We generated this model from the model of *sn*-1-stearoyl-2-arachidonoyl DG by changing the *sn*-2 distal double bond to a single bond and rebalancing hydrogen atoms. The saturated, methyl end of the *sn*-2 chain was adjusted for optimal conformation and fit to the *sn*-1 chain.

sn-*1,2-Distearoyl DG.* We obtained an intermediate *sn*-1,2-dilauroyl DG from the crystal structure of *sn*-1,2-dilauroyl PE (13) simply be removing the head group and refining the model with MMP2 to remove residual strains. These strains arose from two sources: *1*) small uncertainties in experimental atom positions, and *2*) the change from a crystalline solid to an "in vacuo" molecule in the model. The refined *sn*-1,2-dilauroyl DG model showed only minor differences in atomic coordinates compared with the crystal structure of *sn*-1,2-dilauroyl PE (on the order of 0.1 Å units root mean square error). Thus, MMP2 accepted the experimental coordinates as a reasonable approximation to a minimum energy conformation.

We created a model of *sn*-1,2-distearoyl DG by extending the acyl chains of the *sn*-1,2-dilauroyl DG model with saturated segments of *trans* configuration, and reminimizing with MMP2. Congruent portions of the *sn*-1,2-distearoyl DG and *sn*-1,2-dilauroyl DG were similar and the distal segments of the stearoyl chains maintained the all-*trans* conformations and interactions of the proximal segments.

sn-*1-Stearoyl-2-linoleoyl DG.* Linoleic acid contains the minimum number of double bonds required to produce an angle-iron-shaped segment, but also contains two relatively long, saturated segments. On the basis of our experience with previous DG models and a published structure for crystalline linoleic acid (14), we generated a model of this DG that contained a short angle-iron-shaped segment. Note that the angle-iron segment (bonds β-11 to β-14) was a reflected conformation, as had been found optimal for *sn*-1-stearoyl-2-arachidonoyl DG. Furthermore, we adjusted the torsion angles adjacent to the diene segment in our model to values similar to those found to align proximal and distal saturated segments with the tetraene segment in *sn*-1-stearoyl-2-arachidonoyl DG. These torsion angles contrasted to those in crystalline linoleic acid, which produced a jogged conformation (14). Further adjustment of torsion angles near the *sn*-2 chain bend in the model DG brought the dienoic chain roughly parallel to the *sn*-1 chain. Then we used MMP2 to produce a final optimized conformation.

sn-*1-Stearoyl-2-linolenoyl DG.* We generated the model from the *sn*-1-stearoyl-2-linoleoyl DG model by changing the single bond between *sn*-2 carbon atoms 15 and 16 to a double bond and rebalancing hydrogens. We adjusted the new distal double bond to extend the existing angle-iron configuration, and gave the terminal ethyl group the same configuration as the corresponding ethyl group in the *sn*-1-stearoyl-2-docosahexaenoyl DG model.

sn-*1-Stearoyl-2-oleoyl DG.* The model contained an *sn*-2 monoenoic chain that had a kinked conformation based on our previous hydrocarbon modeling (1) and on X-ray diffraction data for oleic acid and cholesteryl oleate (15–18). This chain had a *trans-antiskew-cis-antiskew-antigauche-trans* torsion sequence about the double bond, for bonds β-8 to β-13 (Table 1). We sought to create maximal van der Waals contact between the straight *sn*-1 chain and the kinked *sn*-2 chain by tilting the mean axis of the latter. Such a tilt is implied by the data of Seelig and Waespe-Sarcevic (19). However, MMP2 optimization showed that the molecule resisted being placed in such a conformation.

RESULTS

The principal goals of this study were *1*) to determine how angle-iron-shaped polyene sequences in different *sn*-2-linked fatty acids might affect the conformation of model *sn*-1-stearoyl-2-acyl DGs, and *2*) to compare the conformations of polyenoic DGs with those of monoenoic and disaturated DGs. We therefore constructed a series of *sn*-1-stearoyl-2-acyl DGs containing *sn*-2 chains with 0 to 6 *cis* double bonds (see Methods). We folded all *sn*-2 chain polyene segments into the angle-iron-shaped conformation, adjusted the overall conformations of the DGs to resemble that of the DG backbone in crystalline *sn*-1,2-dilauroyl PE (13), and used the molecular mechanics program, MMP2, to optimize the conformations of the models. This approach led to the identification of three types of DG that had distinctive, energy-minimized conformations.

Type 1 DGs: DGs containing *sn*-2 chains with proximal polyene segments

One type of DG was represented by *sn*-1-stearoyl-2-docosahexaenoyl DG, *sn*-1-stearoyl-2-arachidonoyl DG, and *sn*-1-stearoyl-2-(5,8,11)-eicosatrienoyl DG (**Fig. 1**). The effective dimensions of these DGs were similar, measured for the bounding box defined in **Table 3.** The average values for length, width, and thickness were 29.05 ± 0.02 Å, 10.52 ± 0.16 Å, and 7.18 ± 0.10 Å, respectively. Thus, the gross shapes of the DGs could be approximated by thick rectangular slabs.

The main longitudinal axis of each DG was defined by the glycerol moiety and the *sn*-1-stearoyl chain, which were aligned (Fig. 1). The width and thickness of each DG were determined by the interaction of the *sn*-1 chain with the angle-iron-shaped polyene segment of the *sn*-2 chain. This segment began on carbon 4 of the *sn*-2-docosahexaenoyl chain and on carbon 5 of the *sn*-2-arachidonoyl

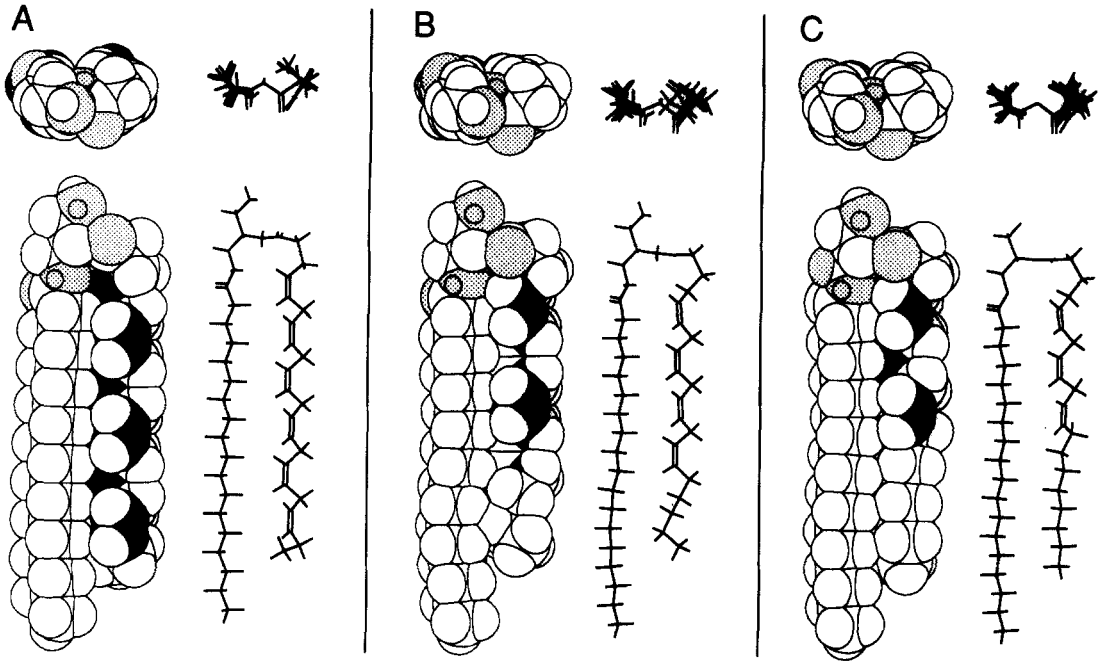

Fig. 1. Conformations of Type 1 *sn*-1-stearoyl-2-acyl-glycerols. MMP2 minimum energy conformations are shown. In each subpanel (A, B, C) the shape and volume of each molecule are shown on the left as space-filling views. Oxygen atoms are emphasized by light gray stippling, and sp^2 (double-bonded) carbon atoms by black shading. The MMP2 data base was used to set Van der Waals radii of atoms. The underlying connectivity and conformation are shown on the right as Dreiding views. The upper views in each subsection show the molecule from the polar end, while the lower views show it from the side containing the ester carbonyl oxygen of the *sn*-2 chain. Panel A, *sn*-1-stearoyl-2-docosahexaenoyl DG; B, *sn*-1-stearoyl-2-arachidonoyl DG; C, *sn*-1-stearoyl-2-(5,8,11)-eicosatrienoyl DG.

and *sn*-2-eicosatrienoyl chains, just after a 90°C bend in the *sn*-2 chain (Fig. 1 A–C). The axis of the polyene segment therefore paralleled that of the *sn*-1 chain at the level of *sn*-1 carbons 1 to 15. The groove formed by the angle-iron-shaped polyene segment faced the *sn*-1 chain and was nearly bisected by a reference plane through the axes of the two chains. The *sn*-1 chain axis with its associated *sn*-1 carbonyl group was rotated by about 30°C with respect to this plane. The methylene hydrogens of the chain then fit well into the groove of the angle-iron. Rotation of the *sn*-1

TABLE 3. Relative shapes and sizes of DG molecules

sn-1-Stearoyl-2-acyl-DG	*sn*-1 Chain Length	*sn*-2 Chain Length	Maximum Width	Maximum Thickness
Type 1				
Docosahexaenoyl	29.03	24.85	10.43	7.06
Arachidonyl	29.04	23.82	10.74	7.18
Eicosatrienoyl (5,8,11)	29.08	24.66	10.39	7.31
Type 2				
Stearoyl	29.10	25.31	10.76	6.39
Linoleoyl	29.28	23.74	11.52	6.43
Linolenoyl	29.22	21.87	11.27	6.55
Type 3				
Oleoyl	28.65	23.38	11.12	8.08

Distances are given in Ångstroms. Molecules were aligned with their acyl chain axes parallel to the Z axis of the coordinate system, with the X axis passing through the 021 atom at the origin and parallel to a plane containing the axes of both chains, and the Y axis perpendicular to X. Chain lengths are measured from the 021 atom of the *sn*-2 ester group along the Z axis to the most distant hydrogen atom of the terminal methyl groups of the *sn*-1 and *sn*-2 chains, respectively. In each case the MMP2 Van der Waals radii of the hydrogen atoms and the 021 oxygen atom were added to the distances. Molecule widths were measured along the X axis between the atoms with the lowest and highest values of the X coordinate. Molecule thicknesses were defined similarly along the Y axis by atoms with the lowest and highest Y coordinates. Again, the appropriate MMP2 Van der Waals radii were added to the distances between atoms.

chain occurred even when the angle-iron-shaped segment was short, as in the case of *sn*-1-stearoyl-2-eicosatrienoyl DG. For this DG only carbons 1–7 of the *sn*-1 chain fit into the groove of the angle-iron. Nevertheless, the remainder of the *sn*-1 chain retained its rotated configuration.

The structural differences between the three DGs did not interfere with their overall conformational characteristics. The *sn*-1-stearoyl-2-docosahexaenoyl DG, reoptimized with the current version of MMP2 to allow comparison with the other DGs, showed the same uniform conformation that we had reported earlier (1). The angle-iron-shaped polyene sequence accounted for the bulk of the *sn*-2 chain, and the short saturated segment at the chain's methyl end tucked into a conformation that matched the cross section of the angle-iron.

The *sn*-1-stearoyl-2-arachidonoyl DG showed a similar conformation after being modified from our previous model of this DG (1) and reoptimized. The double bond sequence in the arachidonoyl chain beginning at carbon 5 required a reflected conformation to join without strain to the chain's bent proximal part. We achieved this conformation by changing the signs of the bond rotations at all methylene groups separating the double bonds (see Methods). The width and alignment of the distal, saturated end of the arachidonoyl chain generally corresponded to that of the angle-iron-shaped polyene segment when we used the sequence of gauche and *trans* rotations for bonds, β-17 to β-20, given in Table 1. These modifications added to the stability of the model and caused the fit between the *sn*-1 and *sn*-2 chains to become as good as that for the reoptimized model of *sn*-1-stearoyl-2-docosahexaenoyl DG.

We used a similar approach to optimize the conformation of the initial part of the *sn*-2 chain of *sn*-1-stearoyl-2-(5,8,11)-eicosatrienoyl DG. As a result, the torsion angles at the bend in the chain and the inverted sequence of torsion angles in the polyene segment were similar to those found for *sn*-1-stearoyl-2-arachidonoyl DG (Table 1). However, the distal methylene torsions in the polyene segment of the eicosatrienoyl chain showed a wider variation from the ideal $\pm$ 120° skew values than that found for the arachidonoyl chain. Furthermore, the configuration of the saturated sequence at the distal end of the eicosatrienoyl chain differed from that of the corresponding sequence in the arachidonoyl chain. Minimum MMP2 energy was obtained with an all-*trans* configuration with the plane of the carbon atoms parallel to that of the *sn*-1 chain carbons. This configuration allowed optimal interdigitation of methyl groups in the distal segments of the *sn*-1 and *sn*-2 chains.

In summary, *sn*-1-stearoyl-2-docosahexaenoyl DG, *sn*-1-stearoyl-2-arachidonoyl DG, and *sn*-1-stearoyl-2-eicosatrienoyl DG could adopt similar, compact low-energy conformations despite their structural differences. Three conformational similarities were particularly noteworthy: *1*) the main axes of the *sn*-2 chains were essentially straight; *2*) the proximally located, angle-iron-shaped polyene sequences in the *sn*-2 chains allowed a special interaction between the *sn*-1 chain and the *sn*-2 chain; and *3*) the *sn*-1 chain with its associated carbonyl group was rotated by about 30°C out of the plane passing through the *sn*-1 and *sn*-2 chain axes. The main conformational difference among the DGs was the steric sense of the angle-irons, with that of the Δ-5 double bond sequence in the arachidonoyl and eicosatrienoyl chains being opposite to that of the Δ-4 sequence in the docosahexaenoyl chain. However, this conformational difference had little effect on the general shape of the DGs and was actually necessary to avoid strains on the internal bonds.

Type 2 DGs: DGs containing *sn*-2 chains with proximal saturated segments

This type of DG was represented by *sn*-1,2-distearoyl DG, *sn*-1-stearoyl-2-linoleoyl DG, and *sn*-1-stearoyl-2-linolenoyl DG (see Methods and Table 1). These DGs all had compact, regular conformations as in the case of the type 1 DGs (**Fig. 2**). However, the shapes of the type 2 DGs differed from those of the type 1 DGs because the *sn*-1 and *sn*-2 chains interacted differently. The effective dimensions for the average length, width, and thickness of the DGs were 29.20 $\pm$ 0.07 Å, 10.63 $\pm$ 0.17 Å, and 6.46 $\pm$ 0.07 Å, respectively (Table 3). Thus the type 2 DGs were slightly wider and somewhat thinner than the type 1 DGs.

In the type 2 DGs, as exemplified by *sn*-1,2-distearoyl DG (see Table 1 and Fig. 2A), the initial segments of both chains were saturated and two configurational features allowed the narrow faces of these segments to interdigitate. The two chains showed nearly equal axial rotations of about 5° to 10° relative to the reference plane through the chain axes. In addition, the plane defined by the *sn*-2 ester carbon and oxygen atoms tilted slightly toward the methyl end of the molecule. Interdigitation along the broad faces of the chains would have produced stronger Van der Waals interactions (and wider and thicker overall molecular dimensions), but would have required closer chain packing than permitted by the *sn*-2 ester geometry.

The interdigitation of the initial segments of the *sn*-1 and *sn*-2 chains was a function of the bond rotation angles in the glyceryl ester region (Table 1) and occurred whether or not the *sn*-2 chains contained distally located polyene segments (compare Figs. 2A, B, and C). The grooves in the short angle-iron-shaped polyene sequences of the linoleoyl and linolenoyl chains were able to accommodate the narrow faces of the *sn*-1 chains without disrupting the axial regularity of the DGs. Thus, no large axial rotation of the *sn*-1 chain was needed to fit either of the short angle-iron segments.

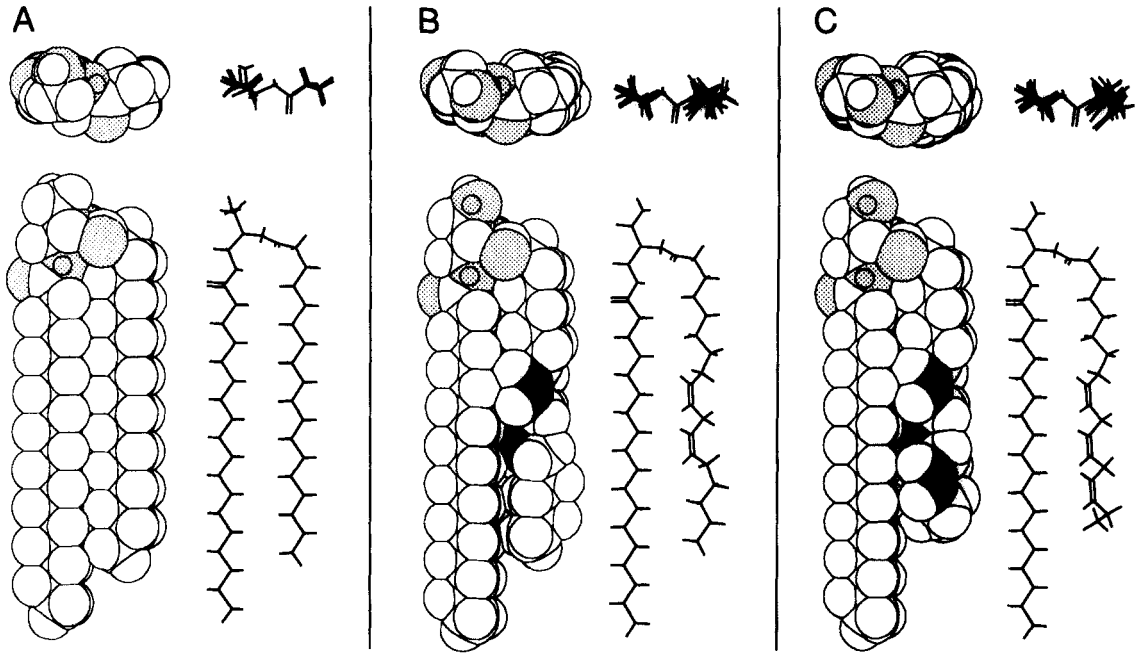

Fig. 2. Conformations of Type 2 *sn*-1-stearoyl-2-acyl-glycerols. The organization of molecule views in subpanels (A, B, C) is the same as for Fig. 1. Panel A, *sn*-1,2-distearoyl DG; B, *sn*-1-stearoyl-2-linoleoyl DG; C, *sn*-1-stearoyl-2-linolenoyl DG.

A sequence of *trans* single bonds at the distal part of the linoleoyl chain gave the lowest-energy conformation, in contrast to the *sn*-1-stearoyl-2-arachidonoyl DG model. The *trans* bonds better fit the less rotated *sn*-1 chain than the more complex folding of the corresponding five-carbon segment in the arachidonoyl chain of *sn*-1-stearoyl-2-arachidonoyl DG (compare Figs. 1B and 2B). The distal saturated segment of the linolenoyl chain folded under one of the angle-iron planes, as did the corresponding segment in *sn*-1-stearoyl-2-docosahexaenoyl DG (compare Figs. 1A and 2C). Nevertheless, the polyenoic, type 2 DGs did show some local increase in the cross-sectional area of the polyene region relative to that of the saturated region. Furthermore, the Van der Waals interaction between the *sn*-1 chain and *sn*-2 chain was reduced compared with that of the type 1 DG interchain packing.

In summary, type 2 DGs had similar, compact conformations whether they contained distal polyene segments or not. These conformations differed from those of group 1 DGs because the initial segments of the two acyl chains in the group 2 DGs were saturated. This allowed the chains to interdigitate, producing a parallel, nearly coplanar orientation of the carbon-atom planes of the initial, saturated chain segments, with the *sn*-1 carbonyl group projecting in the same plane. This had a significant effect on the overall shape of the type 2 DGs, creating a broader molecule than the type 1 DGs, augmented at the ester level by the projection of the bulky *sn*-1 carbonyl group.

Type 3 DGs: DGs containing monoenoic *sn*-2 chains

This type of DG was represented by *sn*-1-stearoyl-2-oleoyl DG (**Fig. 3**). Its conformation was highly irregular, in contrast to the conformations of type 1 and type 2 DGs (compare Figs. 1 and 3). This irregularity was caused by the *sn*-2-oleoyl Δ-9 *cis* double bond. The effect of this bond was reduced but not entirely compensated for by a *trans-antiskew-cis-antiskew-antigauche* sequence (Table 1). The initial, saturated segment of the *sn*-2 chain interdigitated with the *sn*-1 chain and was nearly parallel to it. But the double bond interrupted the interdigitation by displacing the *sn*-2 chain to the side and effectively shortening it by half a methylene unit. That caused the methylenes in the distal saturated segment of the *sn*-2 chain to be located at the same level as the methylenes in the distal part of the *sn*-1 chain. This prevented the two chains from interdigitating effectively at this level, even though both had a *trans* conformation.

The bond rotations that were associated with this conformation combined features found in the two other types of DG (Table 1). The rotations for bonds θ-3 and θ-4 were similar to those observed for type 2 DGs, but those of bonds β-1 to β-3 were more characteristic of type 1 DGs. Bond β-4 had a unique rotational value unlike that of any other type of DG. The *sn*-1 and *sn*-2 ester regions and the *sn*-2 chain-bending region somewhat resembled those of the type 1 models (compare Fig. 3A with Fig. 1A, B, C).

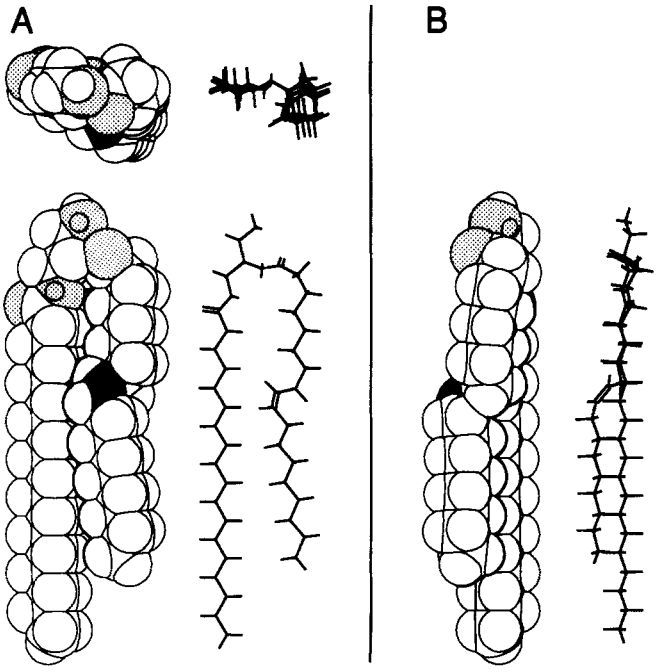

Fig. 3. Conformations of Type 3 *sn*-1-stearoyl-2-acylglycerols. The organization of molecule views in subpanels (A, B) is the same as for Figs. 1 and 2, except that both panels show *sn*-1-stearoyl-2-oleoyl DG. Panel A, the same viewing orientations as in Figs. 1 and 2. Panel B, the molecule has been rotated by 90° about a vertical axis to emphasize the kink in the *sn*-2 chain caused by the isolated double-bond geometry.

However, the proximal portions of both chains tilted slightly relative to the axis defined by the rest of the *sn*-1 chain. These portions of the chains also showed rotated axes somewhat like those of the *sn*-1 chains of type 1 DGs. The net effect was a compromise between maintaining the interdigitation of the proximal saturated segments of the chains and providing space for the jog in the *sn*-2 chain caused by the double bond.

DISCUSSION

The results of this study support three major conclusions. First, *sn*-1-stearoyl-2-acyl DGs that contain *sn*-2-polyunsaturated fatty acyl groups need not have a disordered conformation even when the polyene sequence contains only two *cis* double bonds. Second, these DGs show different compact, energy-minimized conformations depending on the location of the polyene sequence in the *sn*-2-acyl chain. Third, the energy-minimized conformation of *sn*-1-stearoyl-2-oleoyl DG is irregular, even when contacts between the *sn*-1 chain and the *sn*-2 chain are optimized.

The critical feature of polyenoic fatty acids that permits the formation of compact *sn*-1-stearoyl-2-acyl DGs is the ability of their polyene segments to fold into an angle-iron-shaped conformation. Our earlier modeling study demonstrated this feature for docosahexaenoic acid (1). The present study makes a similar point for DGs that contain four other *sn*-2-linked polyunsaturated fatty acyl groups.

The results obtained with *sn*-1-stearoyl-2-eicosatrienoyl DG and *sn*-1-stearoyl-2-linolenoyl DG illustrate a second major point: a proximally located angle-iron-shaped polyene in an *sn*-2 chain is associated with a type 1 DG conformation, whereas a distally located angle-iron-shaped polyene is associated with a type 2 DG conformation (compare Figs. 1C and 2C). The basis for these relationships seems clear. The presence of a proximally located angle-iron-shaped polyene sequence in an *sn*-2 chain promotes one type of acyl chain interaction, while the presence of a proximally located saturated sequence in an *sn*-2 chain promotes another. In particular, the two types of *sn*-2 chain sequence influence the axial rotation of the *sn*-1 chain, which in turn markedly affects the effective width and thickness of the DGs and the orientation of *sn*-1-carbonyl dipoles. The possibility that the proximal part of an *sn*-2 chain may determine the overall conformation of a DG is consistent with reports that proximal chain segments are more ordered than distal ones (20).

The different conformational effects of an angle-iron-shaped polyene sequence and a monounsaturated sequence can be seen from a comparison of the models of *sn*-1-stearoyl-2-linoleoyl DG and *sn*-1-stearoyl-2-oleoyl DG (Figs. 2B and 3). The conformation of the former was compact and regular; that of the latter was not. Thus, it appears that the presence of a second, methylene-interrupted *cis* double bond in a dienoic fatty acid can compensate for the disordering effect of a single *cis* double bond, whereas rotations of adjacent single bonds in a monoenoic fatty acid cannot.

As we report in a companion paper (5), the conformational differences among the three types of DG described here are associated with profound differences in the way the DGs pack together in simulated monolayers.

This investigation was supported by U.S. Public Health Service grant RR-00166 and by the Howard Hughes Medical Institute. We wish to thank the Regional Primate Research Center, University of Washington, for access to the Prophet workstation and to thank the San Diego Supercomputer Center for computing time allocated from a block grant of time assigned to the University of Washington.

Manuscript received 1 April 1991 and in revised form 9 July 1991.

REFERENCES

1. Applegate, K. R., and J. A. Glomset. 1986. Computer-based modeling of the conformation and packing properties of docosahexaenoic acid. *J. Lipid Res.* **27:** 658-680.
2. Allinger, N. L., and Y. H. Yuh. 1981. MM2: Molecular Mechanics II. *Quantum Chemical Program Exchange.* **13:** 395.
3. Allinger, N. L. 1977. Conformational Analysis. 130. MM2.

A hydrocarbon force field utilizing V1 and V2 torsional terms. *J. Am. Chem. Soc.* **99:** 8127–8134.
4. Allinger, N. L. 1976. Calculations of molecular structure and energy by force-field methods. *Adv. Phys. Org. Chem.* **13:** 1–82.
5. Applegate, K. R., and J. A. Glomset. 1991. Effect of acyl chain unsaturation on the packing of model diacylglycerols in simulated monolayers. *J. Lipid Res.* **32:** 0000–0000.
6. BBN Systems and Technologies. 1990. The Prophet Primer. Release 3.1. BBN Systems and Technologies, Cambridge, MA. 1–109.
7. BBN Systems and Technologies. 1990. CAMCRYST. *In* Prophet Molecules. Release 3.1. BBN Systems and Technologies, Cambridge, MA. 240–272.
8. BBN Systems and Technologies. 1990. MMP2MODEL. *In* Prophet Molecules. Release 3.1. BBN Systems and Technologies, Cambridge, MA. 353–357.
9. Allinger, N. L. 1987. Operating Instructions for the MM2 Program, 1987 Force Field. (Available on request from the author.)
10. Sprague, J. T., J. C. Tai, Y. Yuh, and N. L. Allinger. 1987. The MMP2 Computational Method. *J. Computational Chem.* **8:** 581–605.
11. Hauser, H., I. Pascher, and S. Sundell. 1988. Preferred conformation and dynamics of the glycerol backbone in phospholipids: an NMR and X-ray single crystal analysis. *Biochemistry.* **27:** 9166–9174.
12. Hamilton, J. A., S. P. Bhamidipati, D. R. Kodali, and D. M. Small. 1991. The interfacial conformation and transbilayer movement of diacylglycerols in phospholipid bilayers. *J. Biol. Chem.* **266:** 1177–1186.
13. Elder, M., P. Hitchcock, R. Mason, and G. G. Shipley. 1977. A refinement analysis of the crystallography of the phospholipid, 1,2-dilauroyl-DL-phosphatidylethanolamine, and some remarks on lipid-lipid and lipid-protein interactions. *Proc. R. Soc. Lond. A.* **354:** 157–170.
14. Ernst, J., W. S. Sheldrick, and J. H. Fuhrhop. 1979. The structures of the essential unsaturated fatty acids, crystal structure of linoleic acid, as well as evidence for the crystal structure of alpha-linolenic acid and arachidonic acid. *Z. Naturforsch.* **84b:** 701–711.
15. Abrahamsson, S., and I. Ryderstedt-Nahringbauer. 1962. The crystal structure of the low-melting form of oleic acid. *Acta Crystallogr.* **15:** 1261–1268.
16. Craven, B. M., and N. G. Guerina. 1979. The crystal structure of cholesteryl oleate. *Chem. Phys. Lipids.* **24:** 91–98.
17. Gao, Q., and B. M. Craven. 1986. Conformation of the oleate chains in crystals of cholesteryl oleate at 123 K. *J. Lipid Res.* **27:** 1214–1221.
18. Huang, C. H. 1977. A structural model for the cholesterol-phosphatidylcholine complexes in bilayer membranes. *Lipids.* **12:** 348–356.
19. Seelig, J., and N. Waespe-Sarcevic. 1978. Molecular order in *cis* and *trans* unsaturated phospholipid bilayers. *Biochemistry.* **17:** 3310–3315.
20. Seelig, J., and J. L. Browning. 1978. General features of phospholipid conformation in membranes. *FEBS Lett.* **92:** 41–44.
21. Sundaralingam, M. 1972. Molecular structures and conformations of the phospholipids and sphingomyelins. *Ann. NY Acad. Sci.* **195:** 324–355.